Hybridization of Multi-Objective Evolutionary Algorithms and Artificial Neural Networks for Optimizing the Performance of Electrical Drives

Alexandru-Ciprian Zăvoianu [a,c] Gerd Bramerdorfer [b,c] Edwin Lughofer [a] Siegfried Silber [b,c]
Wolfgang Amrhein [b,c] Erich Peter Klement [a,c]

[a] *Department of Knowledge-based Mathematical Systems/Fuzzy Logic Laboratory Linz-Hagenberg, Johannes Kepler University of Linz, Austria*
[b] *Institute for Electrical Drives and Power Electronics, Johannes Kepler University of Linz, Austria*
[c] *ACCM, Austrian Center of Competence in Mechatronics, Linz, Austria*

Abstract

Performance optimization of electrical drives implies a lot of degrees of freedom in the variation of design parameters, which in turn makes the process overly complex and sometimes impossible to handle for classical analytical optimization approaches. This, and the fact that multiple non-independent design parameter have to be optimized synchronously, makes a soft computing approach based on multi-objective evolutionary algorithms (MOEAs) a feasible alternative. In this paper, we describe the application of the well known Non-dominated Sorting Genetic Algorithm II (NSGA-II) in order to obtain high-quality Pareto-optimal solutions for three optimization scenarios. The nature of these scenarios requires the usage of fitness evaluation functions that rely on very time-intensive finite element (FE) simulations. The key and novel aspect of our optimization procedure is the *on-the-fly automated creation of highly accurate and stable surrogate fitness functions* based on artificial neural networks (ANNs). We employ these surrogate fitness functions in the middle and end parts of the NSGA-II run ($\rightarrow$ *hybridization*) in order to significantly reduce the very high computational effort required by the optimization process. The results show that by using this hybrid optimization procedure, the computation time of a single optimization run can be reduced by 46% to 72% while achieving Pareto-optimal solution sets with similar, or even slightly better, quality as those obtained when conducting NSGA-II runs that use FE simulations over the whole run-time of the optimization process.

Key words: electrical drives, performance optimization, multi-objective evolutionary algorithms, feed-forward artificial neural networks, surrogate fitness evaluation, hybridization

1. Introduction

1.1. *Motivation*

Today, electrical drives account for about 70% of the total electrical energy consumption in industry and for about 40% of used global electricity [1]. In [2] it is stated that, each year, in the European Union, the amount of wasted energy that could be saved by increasing the efficiency of electrical drives is around 200TWh and for this reason, in 2009, a European regulation was concluded forcing a gradual increase of the energy efficiency of electrical drives [3]. However, manufacturers of electrical machines need to take more than just the efficiency into account to hold their own value in the global market. To be able to successfully compete, the electrical drives should be fault-tolerant and should offer easy to control operational characteristics and compact dimensions. Apart from these, the most important quality factor is the price. During the development of an electrical machine, a multi-objective optimization approach [4,5] is required in order to address all of the above aspects and to find an appropriate tradeoff between the final efficiency and the cost of the drive.

1.2. *State-of-the-Art in Electrical Drive Design*

In the past, electrical machines were designed by applying a parameter sweep and calculating a maximum of several hundred designs [6]. Calculating a design actually means predicting the operational behavior of the electrical drive for a concrete set of parameter settings. Because of the nonlinear behavior of the materials involved, such a prediction needs to be based on time intensive finite element simulations. This, combined with the need to have

an acceptable duration of the overall analysis, imposed a severe limitation in the number of designs to be calculated. As such, only major design parameters could be taken into consideration and only a rather coarse parameter step size could be applied.

During the last decade, the use of response surface methodology [7], genetic algorithms [8,9], particle swarm optimization [10] and other techniques [11] for the design of electrical machines and the associated electronics has become state-of-the-art. For a detailed comparisons of these modern approaches and additional reviews of the state-of-the-art in electrical drive design, the reader is kindly directed to consult [12–14].

Although the above mentioned search methods have proved to be far more suitable for the task of multi-objective optimization than basic parameter sweeps, they are still plagued by the huge execution times incurred by the need to rely on FE simulations throughout the optimization procedure. The usage of computer clusters where multiple FE simulations can be performed in parallel can partially address this problem, but the following drawbacks still remain severe:

– The FE evaluation of one particular design still takes a long time and conventional methods need to evaluate each individual design.
– There are high costs associated with the usage of computer clustering architectures and various software licenses.

1.3. *Our Approach*

In our attempt to create an efficient optimization framework for electrical drive design, we are exploiting well known and widely applied genetic algorithms used for multi-objective optimization. These specialized algorithms are generally able to efficiently handle several optimization objectives. For us, these objectives are electrical drive target parameters like efficiency, cogging torque, total iron losses, etc. In our implementation, the goal is to minimize all the objectives. If a target needs to be maximized in the design (e.g., efficiency), during the optimization, its negative value is taken to be minimized. The FE simulations required by each fitness function evaluation are distributed over a high throughput computer cluster system. Although it is able to evolve electrical drive designs of remarkable high quality, the major drawback of this initial, and somewhat conventional, optimization approach (**ConvOpt**) is that it is quite slow as it exhibits overall optimization run-times that vary from $\approx$ 44 to $\approx$ 70 hours. As a particular multi-objective genetic algorithm, we employ the well-known and widely used NSGA-II[15].

One main method aimed at improving the computational time of a multi-objective evolutionary algorithm that has a very time-intensive fitness function is to approximate the actual function through means of *metamodels / surrogate models* [16]. These surrogate models can provide a very accurate estimation of the original fitness function at a fraction of the computational effort required by the latter. Three very well documented overviews on surrogate based analysis and optimization can be found in [17], [18] and [19].

In our case, the idea is to substitute the time-intensive fitness functions based on FE simulations with very-fast-to-evaluate surrogates based on highly accurate regression models. The surrogate models act as direct mappings between the design parameters (inputs) and the electric drive target values which should be estimated (outputs). For us, in order to be effective in their role to reduce overall optimization run-time, the surrogate models need to be constructed *on-the-fly, automatically, during the run of the evolutionary algorithm*. This is because they are quite specific for each optimization scenario and each target value (i.e., optimization goal or optimization constraint) that we consider.

In other words, we would like that only individuals (i.e., electrical drive designs) from *the first N generations* will be evaluated with the time-intensive FE-based fitness function. These initial, FE evaluated, electrical drive designs will form a training set for constructing the surrogate models. For the remaining generations, the surrogate models will substitute the FE simulations as the basis of the fitness function. As our tests show, this yields a significant reduction in computation time.

The novelty of our research lies in the analysis of how to efficiently integrate automatically created on-the-fly-surrogate-models in order to reduce the overall optimization run-time without impacting the high quality of the electrical drive designs produced by ConvOpt.

Artificial Neural Networks (ANNs) [20] are among the popular methods used for constructing surrogate models because they possess the universal approximation capability [21] and they offer parameterization options that allow for an adequate degree of control over the complexity of the resulting model. Another advantage of ANNs is the fact that they are known to perform well on non-linear and noisy data [22] and that they have already been successfully applied in evolutionary computation for designing surrogate models on several instances [23,24]. For the purpose of this research, the particular type of ANN we have chosen to use is the multilayered perceptron (MLP). MLP is a popular and widely used neural network paradigm that has been successfully employed to create robust and compact prediction models in many practical applications [25,26]. However, our choice for the MLP is first and foremost motivated by the fact that, for our specific modeling requirements, MLP-bases surrogate models have proved to be both relatively fast and easy to create as well as extremely accurate.

There is a wide choice of methods available for constructing surrogate models. In this paper, we describe in details how we created surrogates based on MLPs, but our hybridization schema itself is general and suitable for a multitude of modeling methods. In Section 5.1 we present results obtained with other non-linear modeling methods that can be used as alternatives for constructing the surrogate mod-

els. These modeling methods are, support vector regression (SVR) [27], RBF networks [28] and a regression orientated adaptation of the instance based learning algorithm IBk [29]. In the aforementioned section, we also further motivate our current preference for MLP surrogate models.

Regardless of the modeling method used, the automatic surrogate model construction phase involves testing different parameter settings (e.g. different number of neurons and learning rates in the case of MLPs, different values of C and γ in the case of SVR), yielding many models with different complexities and prediction behaviors. Given a certain target parameter we propose a new, automated model selection criterion, aimed at selecting the best surrogate to be integrated in the optimization process. The selected surrogate model should deliver the best tradeoff between smoothness, accuracy and sensitivity, i.e., the lowest possible complexity with an above-average predictive quality.

The rest of this paper is organized in the following way: Section 2 presents an overview of multi-objective optimization problems (MOOPs) in general with a special focus on the particular complexities associated with MOOPs encountered in the design and prototyping of electrical drives. Section 3 contains a description of our hybrid optimization procedure (**HybridOpt**) focusing on the creation and integration of the MLP surrogate models. Section 4 provides the description of the experimental setup. Section 5 contains an evaluation of the performance of the hybrid optimization process with regards to the overall run-time of the simulations and the quality of the obtained solutions. Section 6 concludes the paper with a summary of achieved and open issues.

2. Problem Statement

The design of an electrical machine usually comprises at least the optimization of geometric dimensions for a preselected topology. Figure 1 gives the cross-section of an electrical drive featuring a slotted stator with concentrated coils and an interior rotor with buried permanent magnets. The geometric parameters of this assembly are depicted in the figure (d_{si}, b_{st}, b_{ss}. etc.). Depending on the actual problem setting, usually, most of these parameters need to be varied in order to achieve a cheap motor with good operational behavior. Furthermore, due to the fast moving global raw material market, companies tend to investigate the quality of target parameters with regard to different materials. Sometimes, the study of different topologies is also required during the design stage. All these lead to a relatively high number of input parameters for the optimization procedure.

Furthermore, because the behavior of the materials used to construct the electrical drive cannot be modeled linearly, the evaluation of a given design has to be done by using computationally expensive FE simulations. These are solving non-linear differential equations in order to obtain the values of the target parameters associated with the actual

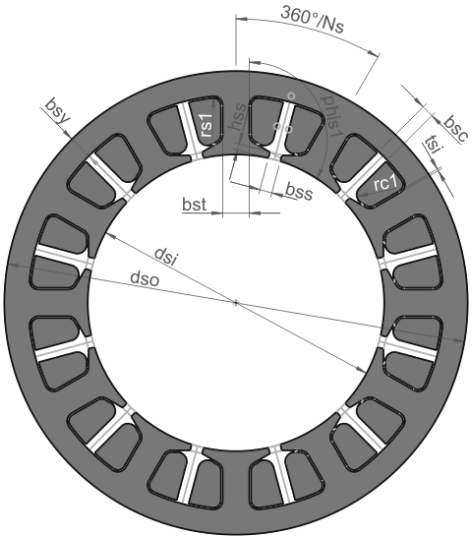

(a) Stator

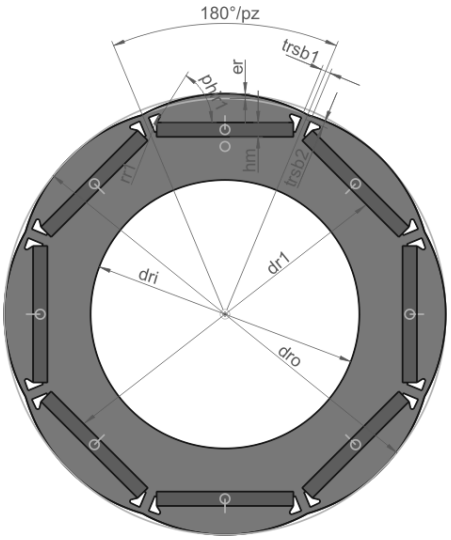

(b) Rotor

Fig. 1. Geometric dimensions of the stator and rotor for an interior rotor topology with embedded magnets

design parameter vector. Specifically, we use the software package FEMAG$^{\mathrm{TM}}$[30] for the calculation of 2D problems on electro-magnetics.

As our main goal is the *simultaneous minimization of all the objectives* (target values) involved, we are faced with a multi-objective optimization problem which can be formally defined by:

$$\min\ (o_1(X), o_2(X), ..., o_k(X)), \tag{1}$$

where

$$o_1(X), o_2(X), ..., o_k(X) \tag{2}$$

are the *objectives* (i.e. target parameters) that we consider and

$$X^T = \left[\begin{array}{cccc} x_1 & x_2 & \dots & x_n \end{array}\right] \tag{3}$$

is the *design parameter vector* (e.g. motor typology identifier, geometric dimensions, material properties, etc).

Additionally, hard constraints like (4) can be specified in order to make sure that the drive exhibits a valid operational behavior (e.g. the torque ripple is upper bound). Such constraints are also used for invalidating designs with a very high price.

$$c(x) \leq 0 \in \mathbb{R}^m \tag{4}$$

In order to characterize the solution of MOOPs it is helpful to first explain the notion of *Pareto dominance* [31]:

Definition 1 *Given a set of objectives, a solution* A *is said to* Pareto dominate *another solution* B *if* A *is not inferior to B with regards to any objectives and there is at least one objective for which* A *is better than* B.

The result of an optimization process for a MOOP is usually a set of Pareto-optimal solutions named the *Pareto front* [31] (a set where no solution is Pareto dominated by any other solution in the set). The ideal result of the multi-objective optimization is a Pareto front which is evenly spread and situated as close as possible to the *true Pareto front* of the problem (i.e., the set of all non-dominated solutions in the search space).

3. Optimization Procedure

3.1. *Conventional Optimization using Multi-Objective Evolutionary Algorithms*

As most evolutionary algorithms (EAs) work generation-wise for improving sets (populations) of solutions, various extensions aimed at making EA populations store and efficiently explore Pareto fronts have enabled these types of algorithms to efficiently find multiple Pareto-optimal solutions for MOOPs in one single run. Such algorithms are referred to as multi-objective evolutionary algorithms or MOEAs in short.

In our case, each individual from the MOEA population will be represented as a fixed length real parameter vector that is actually an instance of the design parameter vector described in (3). Computing the fitness of every such individual means computing the objective functions from (2) and, at first, this can only be achieved by running FE simulations.

The Non-dominated Sorting Genetic Algorithm II (NSGA-II) [15] proposed by K. Deb in 2002 is, alongside with the Strength Pareto Evolutionary Algorithm 2 (SPEA2) [32], one of the most successful and widely applied MOEA algorithms in literature. A brief description of NSGA-II is presented in Appendix A. On a close review, it is easy to observe that both mentioned MOEAs are based on the same two major design principles:

(i) an elitist approach to evolution implemented using a secondary (archiving) population;

(ii) a two-tier selection for survival function that uses a primary Pareto non-dominance metric and a secondary density estimation metric;

In light of the above, it is not surprising that the respective performance of these two algorithms is also quite similar [32,33] with minor advantages towards either of the two methods depending on the particularities of the concrete MOOP problem to be solved [34,35]. Taking into account the similarity of the two MOEAs and the very long execution time required by a single optimization run, we mention that all the tests reported on over the course of this research have been carried out using NSGA-II. Our choice for this method is also motivated by a few initial comparative runs in which the inherent ability of NSGA-II to amplify the search around the extreme Pareto front points enabled it to find a higher number of very interesting solutions than SPEA2 for two of our optimization scenarios.

3.2. *Hybrid Optimization using a Fitness Function based on Surrogate Models*

3.2.1. *Basic Idea*

Our main approach to further improve the run time of the our optimization process is centered on substituting the original FE-based fitness function of the MOEAs with a fitness function based on surrogate models. The main challenge lies in the fact that these surrogate models, which must be highly accurate, are scenario dependent and as such, for any previously unknown optimization scenario, they need to be constructed on-the-fly (i.e., during the run of the MOEA). A sketch of the surrogate-based enhanced optimization process (HybridOpt) outlining the several new stages it contains in order to incorporate surrogate-based fitness evaluation is presented in Figure 2.

In the *FE-based MOEA execution stage* the first N generations of each MOEA run are computed using FE simulations and all the individuals evaluated at this stage will form the training set used to construct the surrogate models. Each sample in this training set contains the initial electrical motor design parameter values (3) and the corresponding objective function values (2) computed using FEMAG$^{\text{TM}}$. Please refer to Section 5.2 for a description of the methodology we used in order to determine a good value of N.

In the *surrogate model construction stage*, we use systematic parameter variation and a selection process that takes into consideration both accuracy and architectural simplicity to find and train the most robust surrogate design for each of the considered target variables.

The next step is to switch the MOEA to a surrogate-based fitness function for the remaining generations that we wish to compute (*surrogate-based MOEA execution stage*). The surrogate-based fitness function is extremely fast when compared to its FE-based counterpart, and it enables the prediction of target values based on input variables within milliseconds. Apart from improving the total run time of the MOEA simulation, we can also take advantage of this massive improvement in speed in two other ways:

(i) by increasing the total number of generations the

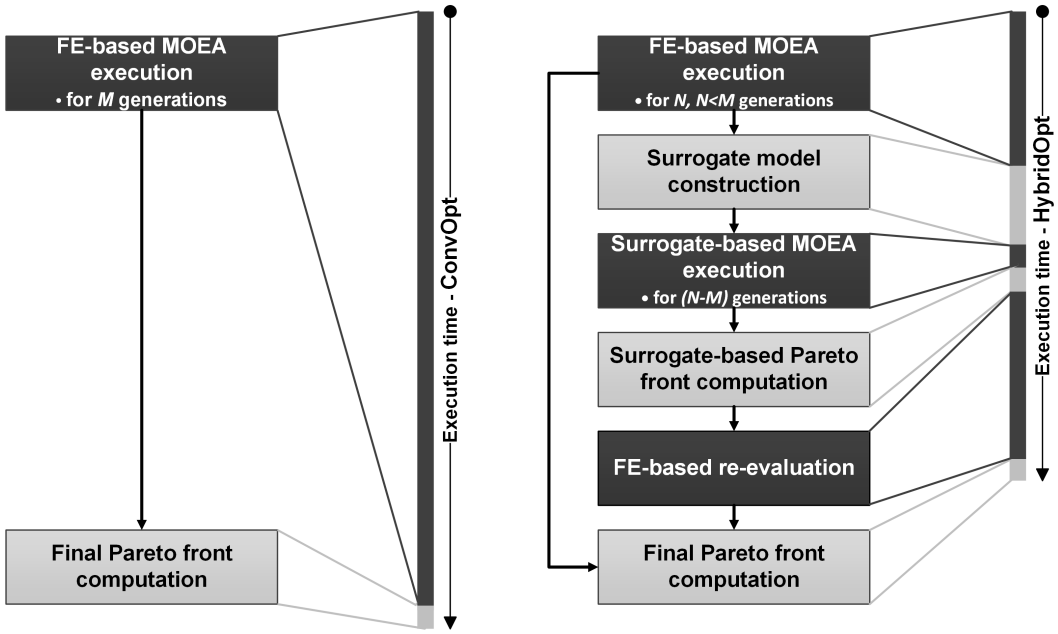

Fig. 2. Diagram of the conventional optimization process - ConvOpt and of the surrogate-enhanced optimization process - HybridOpt when wishing to compute a total of M generations

MOEA will compute during the simulation;

(ii) by increasing the sizes of the populations with which the MOEA operates;

Both options are extremely important as they generally enable MOEAs to evolve Pareto fronts that are larger in size and exhibit a better spread.

In the *surrogate-based Pareto front computation stage* a preliminary surrogate-based Pareto front is extracted only from the combined set of individuals evaluated using the surrogate models. This secondary Pareto front is constructed independently, i.e., without taking into consideration the quality of the FE-evaluated individuals in the first N generations. Initial tests have shown that this approach makes the surrogate-based front less prone to instabilities induced by inherent prediction errors and by the relative differences between the qualities of the surrogate models.

We mention that, in the current stage of development, at the end of the MOEA run (the *FE-based reevaluation stage*), it is desired that all the Pareto-optimal solutions found using the surrogate models are re-evaluated using FE calculations. There are two main reasons for which we do this. The first one is a consequence of the fact that in our optimization framework, the check for geometry errors is tightly coupled with the FE evaluation stage and as such some of the Pareto optimal solutions found using the surrogate models might actually be geometrically invalid. The second reason for the re-evaluation is to assure that all the simulation solutions presented as Pareto optimal have the same approximation error (i.e., the internal estimation error of the FEMAG$^{\mathrm{TM}}$software).

In the *final Pareto front computation stage*, the final Pareto front of the simulation is extracted from the combined set of all the individuals evaluated using FE simulations, i.e., individuals from the initial N generations and FE-reevaluated surrogate-based individuals.

It is important to note that our enhanced optimization process basically redefines the role of the FE simulations. These very accurate but extremely time intensive operations are now used at the beginning of the MOEA driven optimization process, when, generally, the quality-improvement over computation time ratio is the highest. FE simulations are also used in the final stage of the optimization process for analyzing only the most promising individuals found using the surrogate models. In the middle and in the last part of the optimization run, when quality improvements would come at a much higher computational cost, a surrogate-based fitness function is used to steer the evolutionary algorithm.

In the results section, we will show that, using the surrogate enhancement, Pareto fronts with similar quality to the ones produced by ConvOpt can be obtained while significantly reducing the overall simulation time.

3.2.2. *The Structure and Training of ANN Surrogate Models*

Generally, the MLP architecture (Figure 3) consists of one layer of input units (nodes), one layer of output units and one or more intermediate (hidden) layers. MLPs implement the feed-forward information flow which directs data from the units in the input layer through the units in the hidden layer to the unit(s) in the output layer. Any connection between two units u_i and u_j has an associated weight w_{ij} that represents the strength of that respective connection. A concrete MLP prediction model is defined by its specific architecture and by the values of the weights between its units.

Given the unit u_i, the set $Pred(u_i)$ contains all the units u_j that connect to node u_i, i.e. all the units u_j for which w_{ji} exists. Similarly, the set $Succ(u_i)$ contains all the units u_k to which node u_i connects to, i.e. for which w_{ik} exists.

Each unit u_i in the network computes an output value $f(u_i)$ based on a given set of inputs. Depending on how this output is computed, one may distinguish between two types of units in a MLP:

(i) *Input units* - all the units in the input layer. The role of these units is to simply propagate into the network the appropriate input values from the data sample we wish to evaluate. In our case, $f(u_i) = x_i$ where x_i is the i^{th} variable of the design parameter vector from (3).

(ii) *Sigmoid units* - all the units in the hidden and output layers. These units first compute a weighted sum of connections flowing into them (5) and then produce an output using a non-linear logistic (sigmoid shaped) activation function (6):

$$\mathfrak{s}(u_i) = \sum_{u_j \in Pred(u_i)} w_{ji} f(u_j) \tag{5}$$

$$f(u_i) = P(u_i) = \frac{1}{1 + e^{-\mathfrak{s}(u_i)}} \tag{6}$$

In our modeling tasks, we use MLPs that are fully connected, i.e. for every sigmoid unit u_i, $Pred_{u_i}$ exclusively contains all the units in the previous layer of the network. In the input layer, we use as many units as design variables in the data sample. Also, as we construct a different surrogate model for each target variable in the data sample, the output layer contains just one unit and, at the end of the feed-forward propagation, the output of this unit is the predicted regression value of the elicited target (e.g. $P(o_1)$ for the MLP presented in Figure 3).

The weights of the MLP are initialized with small random values and then are subsequently adjusted during a training process. In this training process we use a training set T and every instance (data sample) $\overrightarrow{s} \in T$ contains both the values of the varied design parameters (i.e., X^T) as well as the FE-computed value of the elicited target variable (e.g., $s_{y_{FE}}$ is the FE estimated value of $o_2(X)$ from (2) when $o_2(X)$ is the target for which we wish to construct a MLP surrogate model):

$$\overrightarrow{s} = (x_1, x_2, \ldots, x_n, y_{FE}) \tag{7}$$

The quality of the predictions made by the MLP can be evaluated by passing every instance from the training set through the network and then computing a cumulative error metric (i.e., the batch learning approach). When considering the MLP architecture presented in Figure 3 and the squared-error loss function, the cumulative error metric over training set T is:

$$E(\overrightarrow{w}) = \frac{1}{2} \sum_{\overrightarrow{s} \in T} (s_{y_{FE}} - P(o_1(s_{x_i}, \overrightarrow{w})))^2, i = \overline{1, m} \tag{8}$$

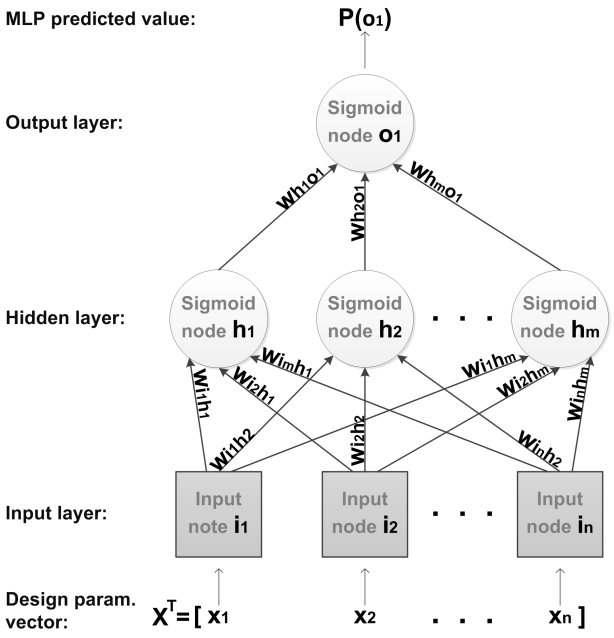

Fig. 3. Multilayer perceptron model with one hidden layer and one output unit

The goal of the training process is to adjust the weights such as to minimize this error metric. The standard approach in the field of ANNs for solving this task is the backpropagation algorithm [36] which is in essence a gradient-based iterative method that shows how to gradually adjust the weights in order to reduce the training error of the MLP.

First, at each iteration t, the error metric $E^t(\overrightarrow{w})$ is computed using (8). Afterwards, each weight w_{ij}^t in the MLP will be updated according to the following formulas:

$$\begin{aligned} \Delta w_{ij}^t &= \eta \delta(u_j) P(u_i) \\ w_{ij}^t &= w_{ij}^t + \Delta w_{ij}^t \quad \text{if } t = 1 \\ w_{ij}^t &= w_{ij}^t + \Delta w_{ij}^t + \alpha \Delta w_{ij}^{t-1} \quad \text{if } t > 1 \end{aligned} \tag{9}$$

where $\eta \in (0, 1]$ is a constant called the *learning rate*. By $\alpha \in [0, 1)$, we mark the control parameter of the empirical enhancement known as *momentum*, which can help the gradient method to converge faster and to avoid some local minima. The function $\delta(u_j)$ shows the cumulated impact that the weighted inputs coming into node u_j have on $E^t(\overrightarrow{w})$ and is computed as:

$$\delta(u_j) = P(u_j)(1 - P(u_j))(y - P(u_j)) \tag{10}$$

if u_j is the output unit and as:

$$\delta(u_j) = P(u_j)(1 - P(u_j)) \sum_{u_k \in Succ(u_j)} \delta_{u_k} w_{jk} \tag{11}$$

if u_j is a hidden unit. The standard backpropagation method proposes several stopping criteria: the number of iterations exceeds a certain limit, $E^t(\overrightarrow{w})$ becomes smaller than a predefined ϵ, the overall computation time exceeds a certain pre-defined threshold. We have chosen to adopt an early stopping mechanism that terminates the execution whenever the prediction error computed over a validation

subset V does not improve over 200 consecutive iterations. This validation subset is constructed at the beginning of the training process by randomly sampling 20% of the instances from the training set T. This stopping criterion may have a benefit in helping to prevent the overfitting of MLP surrogate models.

3.2.3. *The Evaluation and Automatic Model Selection of ANN Surrogate Models*

Usually, in MLP-based data modeling tasks the most important design decision concerns the network architecture: how many hidden layers to use and how many units to place in each hidden layer. In order to construct a highly accurate model, based on the previous architecture choice, one should also experiment with several values for the learning rate and momentum constants. In practice, this problem is most often solved by experimentation usually combined with some sort of expert knowledge.

It has been shown that MLPs with two hidden layers can approximate any arbitrary function with arbitrary accuracy [37] and that any bounded continuous function can be approximated by a MLP with a single hidden layer and a finite number of hidden sigmoid units [38]. The optimization scenarios used in this research (see Section 4.1) do not require the use of two hidden layers. Like with many other interpolation methods, the quality of the MLP approximation is dependent on the number of training samples that are available and on how well they cover the input space. In our application, we have the flexibility to select the number of samples used for training the surrogate model according to the complexity of the learning problem (i.e., number of design parameters and their associated range values) and this aspect is detailed in Section 5.2.

In order to automatically determine the number of hidden units, the learning rate (η) and the momentum (α) needed to construct the most robust MLP surrogate model, we conduct a best parameter grid search, iterating over different parameter value combinations (see Section 4.2 for exact settings).

Our model selection strategy is aimed at finding the most accurate and robust surrogate model where, by robust, we understand a model that displays a rather *low complexity* and a *stable predictive behavior*. Our tests have shown that these two qualities are very important when striving to construct surrogate models that enable the MOEAs to *successfully explore the entire search space*.

The surrogate model selection process (Figure 4) is divided in two stages. In the first stage, all the surrogates are ranked according to a metric that takes into account the accuracy of their predictions. Next, an *accuracy threshold* is computed as the mean of the accuracies of the best performing 2% of all surrogate models. The choice of the final surrogate model is made using a complexity metric that favors the least complex model that has a prediction accuracy higher than the accuracy threshold. The general idea is similar to that of a model selection strategy used for

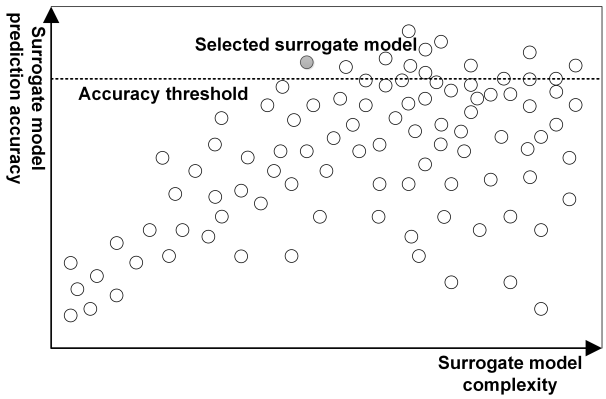

Fig. 4. Diagram of the surrogate model selection process where the predictive accuracy of the model is computed according to (12)

regression trees [39] with the noticeable difference that we compute the accuracy threshold using a broader model basis in order to increase stability (i.e., avoid the cases where the accuracy threshold is solely set according to a highly complex, and possibly overfit, model that is only marginally more accurate than several much simpler ones).

The metric used to evaluate the prediction accuracy of a surrogate model q_m, is based on the coefficient of determination (R^2). In order to evaluate the accuracy of a MLP surrogate model we use a 10-fold cross-validation data partitioning strategy [40] and we compute the value of R^2 over each of the ten folds. The final accuracy assigned to the surrogate model is the mean value of R^2 minus the standard deviation of R^2 over the folds:

$$q_m = \mu(R^2) - \sigma(R^2) \tag{12}$$

Using the standard deviation of R^2 over the cross-validation folds as a penalty in (12) has the role of favoring models that exhibit a more stable predictive behavior. The reason for this is that a significant value of $\sigma(R^2)$ indicates that the surrogate model is biased toward specific regions of the search space. The existence of locally-biased surrogate models is quite probable because our training data is rather unbalanced as it is the byproduct of a highly elitist evolutionary process that disregards unfit individuals.

The second metric used in the surrogate model selection process favours choosing less complex models. One MLP surrogate model is considered to be more complex than another if the former has more units in the hidden layer (ties are broken in favor of the model that required more computation time to train).

It is worth mentioning that this automatic surrogate model selection strategy can easily be adapted when opting for another surrogate modeling method. In this case, one only needs to choose a different indicator (or set of indicators) for measuring complexity (e.g. the C parameter and/or the number of required support vectors in the case of a SVR).

Algorithm 1 Description of the hybrid optimization process

1: **procedure HybridOpt**($Scenario, PopSize_{ini}, PopSize_{ext}, N, M$)
2: $P \leftarrow$ RandomlyInitializePopulation($Scenario, PopSize_{ini}$)
3: $E \equiv$ FE-Evaluator($Scenario$)
4: $\langle P, Valid_{FE} \rangle \leftarrow$ **NSGA-II-Search**($N, PopSize_{ini}, P, E$)
5: $Configurations \leftarrow$ InitializeMlpGridSearchConfigurations
6: **for all** $target \in Scenario$ **do**
7: $Map \leftarrow \emptyset$
8: **for all** $c \in Configurations$ **do**
9: $Map \leftarrow Map \cup$ ConstructSurrogateModel($c, target, Valid_{FE}$)
10: **end for**
11: $BestSurrogateModels(target) \leftarrow$ SelectBestSurrogateModel(Map)
12: **end for**
13: $E \equiv$ SurrogateEvaluator($Scenario, BestSurrogateModels$)
14: $\langle P, Valid_{MLP} \rangle \leftarrow$ **NSGA-II-Search**($M - N, PopSize_{ext}, P, E$)
15: $OptimalSet_{MLP} \leftarrow$ ExtractParetoFront($Valid_{MLP}$)
16: $E \equiv$ FE-Evaluator($Scenario$)
17: $OptimalSet_{MLP} \leftarrow$ EvaluateFitness($OptimalSet_{MLP}, E$)
18: **return** ExtractParetoFront($Valid_{FE} \cap OptimalSet_{MLP}$)
19: **end procedure**

20: **function NSGA-II-Search**($NrGen, PopSize, InitialPopulation, FitnessEvaluator$)
21: $t \leftarrow 1$
22: $ValidIndividuals \leftarrow \emptyset$
23: $P(t) \leftarrow InitialPopulation$
24: $P(t) \leftarrow$ EvaluateFitness($P(t), FitnessEvaluator$)
25: **while** $t \leq NrGen$ **do**
26: $O(t) \leftarrow$ CreateOffspring($P(t), PopSize$)
27: $O(t) \leftarrow$ EvaluateFitness($O(t), FitnessEvaluator$)
28: $ValidIndividuals \leftarrow ValidIndividuals \cup O(t)$
29: $P(t+1) \leftarrow$ ComputeNextPopulation($P(t), O(t), PopSize$)
30: $t \leftarrow t + 1$
31: **end while**
32: **return** $\langle P(t), ValidIndividuals \rangle$
33: **end function**

3.2.4. *Algorithmic Description of HybridOpt*

Our hybrid optimization procedure is presented in Algorithm 1. Apart from method calls and the normal assignment operator ($\leftarrow$), we also use the operator $\equiv$ in order to mark the dynamic binding of a given object to a specific method with the implied meaning that all future references to the object are redirected to the corresponding targeted method.

The main procedure, named HybridOpt, has five input parameters:

- *Scenario* - the description of the scenario to be optimized with information regarding design parameters and targets
- $PopSize_{ini}$ - the size of the NSGA-II population for the FE-based part of the run
- $PopSize_{ext}$ - the size of the NSGA-II population for the surrogate-based part of the run
- N - the number of generations to be computed in the FE-based part of the run
- M - the total number of generations to be computed during the optimization (i.e., $M - N$ generations will be computed in the surrogate-based part)

The NSGA-II implementation contained in the NSGA-II-Search function differs from standard implementations as it returns two results, the Pareto optimal set obtained after constructing the last generation and a set containing all the *valid* individuals generated during the search. This function has four input parameters:

- *NrGen* - the number of generations to be computed
- *PopSize* - the size of the population
- *InitialPopulation* - a set containing the starting population of the evolutionary search
- *FitnessEvaluator* - an object that is bound to a specific fitness evaluation function

The method EvaluateFitness is of particular importance. It receives as input a set of unevaluated individuals and an object that is bound to a specific fitness evaluation function. EvaluateFitness returns a filtered set containing only the *valid* individuals. Each individual in the returned set also stores information regarding its fitness over

the multiple objectives — note that the fitness is directly associated with the values of the target parameters, which are either predicted by the surrogate model or calculated using differential equations in the FE simulation. If the concrete fitness function used is FE-EVALUATOR, individuals are checked for validity with regards to both geometrical (meshing) errors and constraint satisfaction (4). Geometrical errors may arise because of specific combinations of design parameter values. When using the SURROGATEEVALUATOR, only constraint satisfaction validity checks can be performed.

The other methods that we use in HYBRIDOPT are:

- RANDOMLYINITIALIZEPOPULATION - this method randomly initializes a set of individuals of a given size according to the requirements of the optimization scenario to be solved
- INITIALIZEMLPGRIDSEARCHCONFIGURATIONS - this method constructs all the MLP training configurations that are to be tested in a best parameter grid search (see Section 4.2 for details)
- CONSTRUCTSURROGATEMODEL - this method builds a single MLP surrogate model for a given target based on a preset MLP training configuration and a training set of previously FE-evaluated individuals as described in Section 3.2.2
- SELECTBESTSURROGATEMODEL - this method selects the most robust surrogate from a given set of models according to the surrogate model selection process described in Section 3.2.3
- EXTRACTPARETOFRONT - this method extracts the Pareto-optimal front from a given set of possible solutions after the description in Section 3.1.

In the NSGA-II-SEARCH method, the functions CREATEOFFSPRING and COMPUTENEXTPOPULATION are responsible for implementing the evolutionary mechanism described in Appendix A.

4. Experimental Setup

4.1. *The Optimization Scenarios*

We consider three multi-objective optimization scenarios coming from the field of designing and prototyping electrical drives:

The first scenario (Scenario *OptS1*) is on a motor for which the rotor and stator topologies are shown in Figure 1. The design parameter vector has a size of *six* and is given by

$$\mathbf{X}^T = \left[\begin{array}{cccccc} h_m & \alpha_m & e_r & d_{si} & b_{st} & b_{ss} \end{array} \right] ,$$

where all parameters are illustrated in Fig. 1 except for α_m, which denotes the ratio between the actual magnet size and the maximum possible magnet size as a result of all other geometric parameters of the rotor. The targets for the MLP surrogate model construction stage are the four, unconstrained, Pareto objectives:

- $T1 = -\eta$ - where η denotes the efficiency of the motor. In order to minimize the losses of the motor, the efficiency should be maximized and therefore $-\eta$ is selected for minimization.
- $T2 = T_{cogPP}$ - the peak-to-peak-value of the motor torque for no current excitation. This parameter denotes the behavior of the motor at no-load operation and should be as small as possible in order to minimize vibrations and noise due to torque fluctuations.
- $T3 = TotalCosts$- the material costs associated with a particular motor. Obviously, minimizing this objective is a very important task in most optimization scenarios.
- $T4 = T_{rippPP}$ - the equivalent of $T_{cog,PP}$ at load operation. The values of this objective should also be as small as possible.

The second problem (Scenario *OptS2*) is on an electrical machine featuring an exterior rotor. The design parameter vector contains *seven* geometric dimensions. The aim of this optimization problem was to minimize the total losses of the system at load operation and to minimize the total mass of the assembly while simultaneously maintaining other desired operational characteristics (e.g., efficiency, cogging torque, costs, etc). In the case of this scenario, the first target ($T1$) is a hard-constrained Pareto optimization goal, the second ($T2$) is an unconstrained Pareto optimization goal, whilst the third ($T3$) is a secondary hard constraint imposed on the evolved motor designs.

The third problem (Scenario *OptS3*) also concerns a motor with an exterior rotor. The design parameter vector has a size of *ten*. This scenario proposes four, hard-constrained, Pareto optimization goals. All of them are considered targets in the surrogate model construction phase:

- $T1 = l_s$ - the total axial length of the assembly
- $T2 = TotalMass$ - the total mass of the assembly
- $T3 = P_{Cu}$- the ohmic losses in the stator coils
- $T4 = P_{fe}$ - the total losses due to material hysteresis and eddy currents in the ferromagnetic parts of the motor

4.2. *The Testing Framework*

In order to compare the performance of the two optimization processes we are using optimization runs that compute 100 generations with a population size of 50. This rather small choice of the population size is motivated by restrictions regarding time and the available cluster computation power for running the required simulations.

In order to illustrate some immediate benefits of using the enhanced approach (see Section 3.2.1), we also performed tests where, during the run of the MOEA, after the construction of the mappings, we doubled the population size and the number of generations to be evolved.

Our optimization framework uses the NSGA-II implementation provided by the jMetal package [41]. For all tests reported in Section 5, we used NSGA-II with a crossover probability of 0.9, a crossover distribution index of 20, a mutation probability of $1/|X^T|$ and a mutation distribu-

tion index of 20. The high values of the distribution indexes for the crossover and mutation operators (that are recommended by literature [15] and set as default in jMetal) force NSGA-II to generate near parent values for almost all spawned offspring. While this parameter choice seems to determine an overall search strategy that favors exploitation over exploration, the highly elitist nature of NSGA-II coupled with the high mutation probability, help to balance the exploitation versus exploration ratio over the entire run. Using ConvOpt, we have performed a tuning phase to check whether smaller values (i.e., 15, 10, 5 and 2) for the crossover and mutation distribution indexes would yield better results when using a population size of 50 and a limited number of evolved generations. The results showed that using these smaller index values does not produce any improvement.

In the case of HybridOpt, we perform the mapping training stage after $N = 25$ generations (please see Section 5.2 for a detailed explanation of this parameter choice). As we use a population size of 50, the maximum possible size of the training sets is 1250 samples. The size of the actual training sets we obtained was smaller because some of the evolved design configurations were geometrically unfeasible or invalid with regards to given optimization constraints. When considering all the performed tests, the average sizes and standard deviations of the obtained training sets is presented in Table 1.

Table 1
The average size and standard deviations of the obtained training sets.

Scenario	Training set size μ	Training set size σ
OptS1	1219.50	22.40
OptS2	813	123.59
OptS3	743.25	74.33

The MLP implementation we used for our tests is largely based on the one provided by the WEKA open source machine learning platform [42]. In the case of the best parameter grid searches that we performed in order to create the MLP surrogate models:

- the number of hidden units was varied between 2 and double the number of design variables;
- η was varied between 0.05 and 0.40 with a step of 0.05
- α was varied between 0.0 and 0.7 with a step of 0.1

The search is quite fine grained as it involves building between 704 (scenario *OptS1*) and 1216 (scenario *OptS3*) MLP surrogate models for each elicited target. This approach is possible because we make use of the early stopping mechanism in the MLP training process (see Section 3.2.2) which in turn ensures an average surrogate model training time of 356.70 seconds. We achieve a considerable speedup in the surrogate model creation stage by distributing all the MLP training tasks over the same high throughput cluster computing environment that is used to run in parallel the FE simulations. As a result, the surrogate model creation stage took, on average, 146.33 minutes, over all performed tests.

4.3. *Considered Performance Metrics*

In order to compare the performance and behavior of the conventional and hybrid optimization processes we use four performance metrics:

(i) the hypervolume metric $\mathcal{H}$ [43] measures the overall coverage of the obtained Pareto set;
(ii) the generalized spread metric $\mathcal{S}$ [44] measures the relative spatial distribution of the non-dominated solutions;
(iii) the FE utility metric $\mathcal{U}$ offers some insight on the efficient usage of the FE evaluations throughout the optimization;
(iv) the run-time metric $\mathcal{T}$ records the total runtime in minutes required by one optimization;

The hypervolume and generalized spread metrics are commonly used in MOEA literature when comparing between different non-dominated solution sets. The $\mathcal{H}$ metric has the added advantage that it is the only MOEA metric for which we have theoretical proof [45] of a monotonic behavior. This means that the maximization of the hypervolume constitutes the necessary and sufficient condition for the set of solutions to be *"maximally diverse Pareto optimal solutions of a discrete, multi-objective, optimization problem"*. By design, the upper bound of $\mathcal{H}$ is 1.00. For any optimization problem, the *true Pareto front* yields the highest $\mathcal{H}$ value. As we are not dealing with artificial problems, for our considered scenarios, the best possible value of $\mathcal{H}$ for each problem is unknown.

In the case of the $\mathcal{S}$ metric, a value closer to 0.0 indicates that the solutions are evenly distributed in the search space. Although this metric is not monotonic in showing true Pareto front convergence, in our case, it is extremely useful as it is a good indicator of the diversity of Pareto-optimal electrical drive designs that our optimization runs are able to find.

The FE utility metric is constructed for the purpose of illustrating how efficiently the optimization process is using the very time intensive FE simulations over an entire run. The $\mathcal{U}$ metric is computed as the ratio between the total number of non-dominated solutions found during the optimization (i.e. the size of the final Pareto front) and the total number of performed FE simulations.

5. Results

5.1. *Overview of MLP Surrogate Model Performance*

In order to offer a quick insight into the characteristics of the elicited target variables, Table 3 contains the comparative results of trying to model the targets using linear regression, MLPs and three other non-linear modeling methods. We considered sets containing all the samples obtained

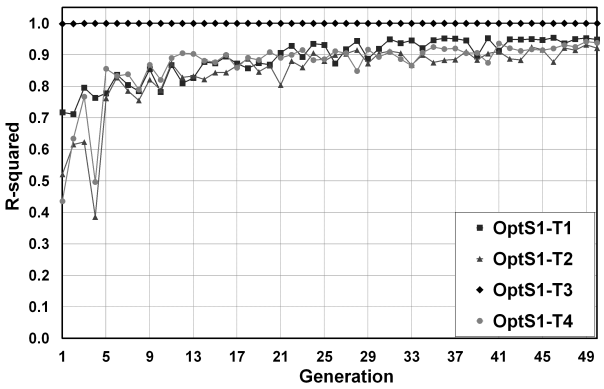

(a) Scenario *OptS1*

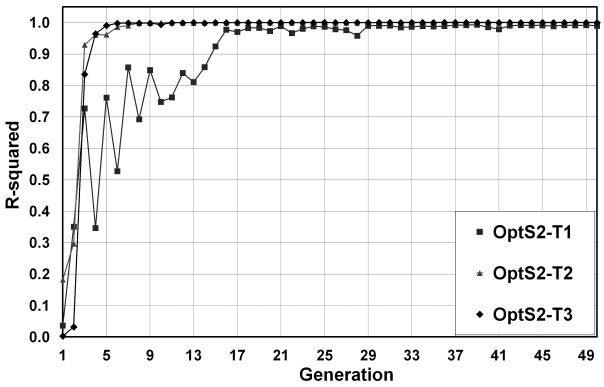

(b) Scenario *OptS2*

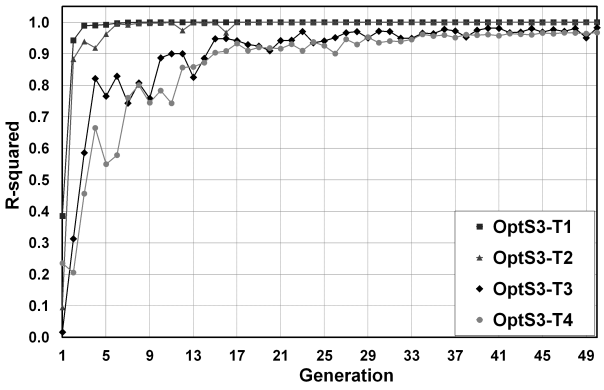

(c) Scenario *OptS3*

Fig. 5. Evolution of the coefficient of determination computed over the remaining $100-n$ generations for the best MLP surrogate models trained using the first $n \leq 50$ generations

using FE simulations over 100 NSGA-II generations with a population size of 50 and split them into training and test data sets. The training data sets contain the individuals from the first 33 generations while the test data sets are made up from the individuals from the last 67 generations (i.e., a "1/3 - training , 2/3 - test" data set partitioning scheme). After removing the geometrically unfeasible and invalid designs, we ended up with training sets of size 1595 (*OptS1*), 1197 (*OptS2*), and 1103 (*OptS3*).

For the non-linear modeling methods, we report the test result achieved by the best surrogate model which was selected based on 10-fold cross-validation performance after doing a best parameter grid search on the training data. In the case of the MLP, the grid search was set up as described in Section 4.2. In the case of SVR, we trained 675 surrogate models for each target as we varied: the general complexity parameter C between $[2^{-4}, 2^{-3}, ..., 2^{10}]$, the RBF kernel parameter γ between $[2^{-5}, 2^{-4}, ..., 2^{3}]$ and the ϵ parameter of the ϵ-intensive loss function between $[0.001, 0.005, 0.01, 0.025, 0.05]$. For RBF networks, we trained 918 surrogate models for each target by varying the number of clusters between $[2, 3, 4, 5, 10, 20, ..., 500]$ and the allowed minimum standard deviation for the clusters between $[0.25, 0.5, 1.00, 2.00, ...15.0]$. When using IBk modeling, we created 900 surrogate models for each target as we varied the number of nearest neighbors from 1 to 300 and we used three different distance weighting options: no weighting, weight by 1/distance and weight by 1-distance.

Firstly, one can observe that while most targets display a strong linear dependency towards their respective design variables, the surrogate models obtained using linear regression for some targets (e.g., *OptS1-T1*, *OptS1-T2*, *OptS1-T4*, *OptS3-T4*) are by no means accurate. For the purpose of this research, we decided on a linear regression R^2 threshold value of 0.9 in order to classify a target as linear or non-linear.

When considering only the six non-linear targets, MLPs and SVR are the best performers (MLP slightly better than SVR) while RBF networks produce results that are significantly worse. We conducted all the best parameter grid searches by distributing the surrogate model training tasks over the computer cluster. We measured the time required by the grid searches conducted for non-linear targets and, for each modeling method, averaged it over the total number of surrogate models to be trained. We present these results in Table 2 and, together with some model complexity information, they indicate that, when comparing with the MLP:

- RBF networks and SVR require $\approx 15\%$ and $\approx 55\%$ more (wall) time in order to finish the grid search.
- when taking into acount the sizes of the training sets, RBF networks and SVR seem to produce surrogate models that are quite complex (i.e., number of clusters required by the RBF network and number of support vectors used by SVR)

The difference in required training time, the low structural complexity, and the higher accuracy motivate our choice of using MLP surrogate models.

5.2. *The Accuracy and Stability of MLP Surrogate Model Predictions*

In the current version of HybridOpt, it is very important to choose a good value for the parameter N that indicates for how many generations we wish to run the initial FE-based execution stage. A value of the parameter that is too low will result in creating inconclusive training sets which

Table 2
Information regarding the average training time of the surrogate models and the structural complexity (i.e., *number of hidden units* in the case of MLP, *number of support vectors* in the case of SVR and *number of clusters* in the case of RBF networks) of the best surrogate model on the non-linear targets

Target	Average training time [minutes]			Complexity indicator of the best surrogate		
	MLP	SVR	RBF Nets	MLP	SVR	RBF Nets
OptS1-T1				11	892	500
OptS1-T2	**0.734**	1.241	0.865	12	754	500
OptS1-T4				11	1046	500
OptS2-T1	0.678	0.931	**0.620**	9	323	300
OptS3-T3	**0.601**	0.945	0.837	12	858	400
OptS3-T4				10	868	400
All non-linear	**0.671**	1.039	0.774	10.83	790.16	433.33

Table 3
Linear and non-linear regression modeling results on the elicited targets

Scenario	Target	Classification	R^2 on test instances				
			Linear	MLP	SVR	RBF Nets	IBk
OptS1	T1	non-linear	0.7353	**0.9864**	0.9330	0.9029	0.8744
	T2	non-linear	0.6048	0.9530	**0.9540**	0.8992	0.9040
	T3	linear	0.9777	0.9992	0.9997	**0.9999**	0.9660
	T4	non-linear	0.6390	**0.9674**	0.9640	0.9099	0.9044
OptS2	T1	non-linear	0.8548	0.9923	**0.9960**	0.9859	0.9749
	T2	linear	0.9916	0.9997	0.9997	**0.9998**	0.9904
	T3	linear	0.9990	**0.9999**	0.9998	**0.9999**	0.9254
OptS3	T1	linear	0.9970	**0.9999**	0.9997	**0.9999**	0.9689
	T2	linear	0.9514	0.9998	0.9995	**0.9999**	0.8822
	T3	non-linear	0.8526	0.9799	**0.9839**	0.9804	0.8791
	T4	non-linear	0.8355	**0.9564**	0.9552	0.9521	0.8794
Average	All	linear	0.9830	**0.9997**	0.9997	**0.9997**	0.9466
Average	All	non-linear	0.7540	**0.9720**	0.9640	0.9384	0.9026
Average	All	all	0.8580	**0.9847**	0.9802	0.9664	0.9226

in turn will lead to surrogate models that are not globally accurate or stable. By choosing a value for N that is a lot higher than the optimal one, we are more or less "wasting" FE simulations by creating oversized training sets. In order to choose a good value of N we take into account the influence that this parameter has on the accuracy and stability of the resulting MLP surrogate models.

In order to estimate the influence that N has on the accuracy of the surrogate models, for each optimization scenario we consider fully FE-based runs of 100 generations and the combined pools of samples that each such simulation produces. We construct 50 different test cases and, for each target of each scenario, we divide the available samples into a training and a test set. For test number i, the training set contains the individuals from the first i generations and the validation set contains the individuals from the last $100 - i$ generations. For each test, we use the best parameter grid search and the automated model selection strategy in order to obtain the best MLP surrogate model on the training data. Next, we evaluate the quality of this surrogate model by computing the coefficient of determination over the corresponding test set. The resulting values are plotted in Figure 5. It can be easily observed that all targets display a stable logarithmic saturation behavior that suggests that a choice of N in the 20 to 30 generations range should be able to produce highly accurate surrogate models for all considered targets.

The concrete decision for the value of N is based on the stability over time of the obtained surrogate models. We estimate the stability over time by computing the individual R^2 of every generation in the test data sets. For example, Figure 6 contains the plots of the generational coefficients of determination for the most difficult to model targets of scenarios *OptS1* and *OptS3* (i.e., *OptS1-T2* and *OptS3-T4*). We are only interested in the best surrogate models constructed using the samples from the first 20 to 30 gen-

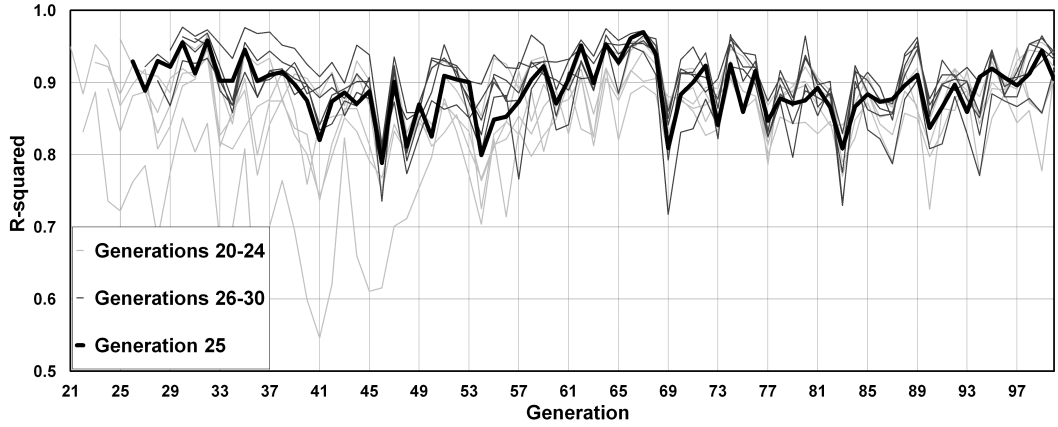

(a) Target *OptS1-T2*

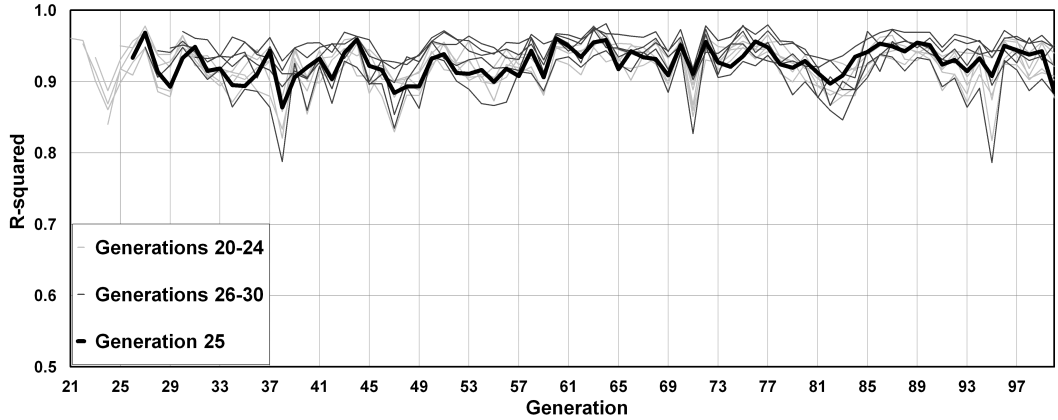

(b) Target *OptS3-T4*

Fig. 6. Evolution of the generational coefficient of determination for MLP surrogate models trained using the first 20 to 30 generations for the most difficult to model targets

erations.

Finally, we have chosen $N = 25$ as this is the *smallest value of N for which the trained surrogate models exhibit both a high prediction accuracy as well as a high prediction stability*. Over all three data sets and the 6 non-linear targets, the generational coefficients of determination (for generations 31 to 100) obtained by the surrogate models constructed using samples from the first 25 generations:

– are higher than 0.9 in 94.52% of the cases;
– are higher than those obtained by the surrogate models constructed using 20-24 generations in 57.52% of the cases and by those obtained by the surrogate models constructed using 26-30 generations in 42.52% of the cases;

All HybridOpt tests reported in the next section have been performed with the parameter setting of $N = 25$.

5.3. *The Comparative Performance of HybridOpt*

In Table 4 we present the comparative performance of ConvOpt and HybridOpt after runs of 100 generations each. The results for each scenario are averaged over five independent runs. For these tests, the size of the population in HybridOpt was fixed, throughout the simulation, to 50 individuals. The performance of our method is very good for scenarios *OptS1* and *OptS2* as the resulting final Pareto fronts have comparable hypervolumes, better spreads and were computed $\approx 63\%$ and $\approx 72\%$ faster than their counterparts.

On the highly constrained scenario *OptS3*, the enhanced optimization process is a little bit worse. The main reason for this is that the hard constraints determine a high ratio of geometrically invalid individuals to be generated during the surrogate-based evaluation stage. However, the computation time could still be reduced by $\approx 46\%$. Even though for this scenario, ConvOpt produces pareto fronts with a better $\mathcal{H}$, HybridOpt is still able to evolve well balanced individual solutions in key sections of the Pareto front — please see Figure 7 for two such examples: the black dots denote solutions obtained from HybridOpt and some of them are very well placed with regards to the origin of the projected Pareto space.

When increasing the size of the population and the number of generations to be computed (in the surrogate-based MOEA execution stage of HybridOpt), the results of the enhanced optimization process are much improved (please see Table 5 for details). In this case, for scenarios *OptS1* and *OptS2*, HybridOpt surpasses ConvOpt with regards to

all the considered performance metrics.

In the case of scenario *OptS3*, the increase of the post-surrogate-creation population and of the number of generations to be evaluated enable HybridOpt to surpass ConvOpt with regards to the spread of the generated Pareto fronts. The hyper-volume values, although much better, are still 4-8% worse than those of ConvOpt.

As the increase in population size and number of generations is directly translated into a higher number of individuals that need to be re-evaluated using FE-simulations, the improvement in computation time is reduced to values ranging from $\approx$ 14% to $\approx$ 69%. The reduction is particularly visible in the case of the hard-constrained scenario *OptS3*, where the amount of geometrically invalid individuals generated in the surrogate-based execution stage also grows substantially.

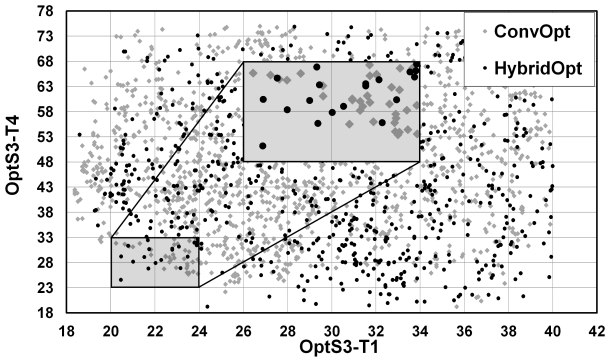

(a) Pareto front nr. 1

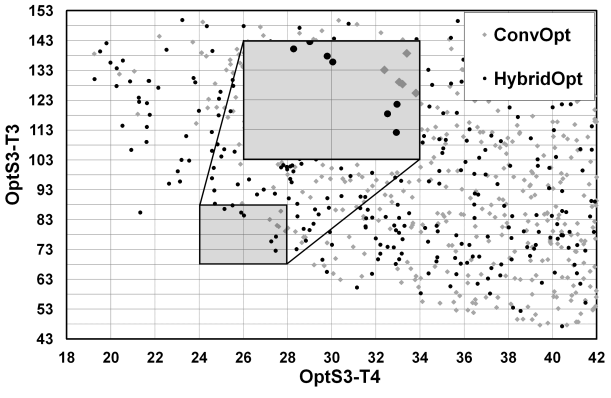

(b) Pareto front nr. 2

Fig. 7. 2D projections of the full Pareto fronts generated using ConvOpt and HybridOpt for the highly constrained scenario *OptS3*. The regions of the fronts with well balanced Pareto optimal designs are magnified.

6. Conclusion

In this paper, we investigated multi-objective optimization algorithms based on evolutionary strategies, exploiting concepts from the famous and widely used NSGA-II algorithm, for the purpose of optimizing the design of electrical drives in terms of efficiency, costs, motor torque behavior, total mass of the assembly, ohmic losses in the stator coils and others. Despite the parallelization of the whole optimization process over a computer cluster, as both the design and the target parameter space can be quite large, very long optimization runs are required in order to solve the complex scenarios that we deal with. This is because the fitness function used by NSGA-II search requires very time-intensive FE simulations in order to estimate the quality of a given motor design.

In order to alleviate the problem, we experimented with a system that automatically creates, on-the-fly, non-linear surrogate models that act as direct mappings between the design and the target parameters of the electrical drive. These surrogate models form the basis of a very fast to surrogate fitness function that replaces the original FE-based fitness for the latter part of the optimization process. Empirical observations over averaged results indicate that this leads to a reduction of the total run-time of the optimization process by 46-72%. For setting up the non-linear surrogate models, we applied multi-layer perceptron (MLP) neural networks, as they turned out to be more efficient in terms of accuracy versus training and evaluation time than other soft computing techniques.

The tests that we have performed show that, on average, the Pareto fronts obtained using the hybrid, surrogate-enhanced approach, are similar (or even slightly better) than those obtained by using the conventional NSGA-II optimization process, which uses only the FE-based fitness evaluation function. This may come as a surprise because when we shift the optimization process to the surrogate-based fitness function, the optimization algorithm will in fact try to converge to a new, surrogate-induced, artificial optimum. The high quality of the MLP surrogate models we obtain directly translates into the fact that the artificial optimum lies in the vicinity of the true (FE-induced) optimum. The close proximity of the two optima is the likely reason for which the surrogate models are always able to efficiently steer the optimization process towards exploring high-quality Pareto fronts (as the results in Section 5.3 indicate).

Future work will basically focus on two issues:

(i) Reducing the importance and the sensitivity of the N parameter in HybridOpt by shifting our optimization algorithm towards an active learning approach. The idea is that initial surrogate models may be set up from fewer generations, than the currently suggested 25 and, from time to time, during the surrogate-based MOEA execution stage, certain individuals (or generations) are to be evaluated by FE-simulations. This dual evaluation (surrogate and FE-based) will provide information for the dynamic adaption of the surrogate models during the run in order to keep (or bring) the quality of these models on a high level throughout the optimization. In fact, an adaptation is very important when some drifts occur in the optimization process [46], in order to omit time-intensive model re-training and evaluation phases. Active learning steps [47] may be essential

Table 4
The averaged performance over five runs of the conventional and hybrid optimization processes

Metric	Scenario *OptS1*		Scenario *OptS2*		Scenario *OptS3*	
	ConvOpt	HybridOpt	ConvOpt	HybridOpt	ConvOpt	HybridOpt
$\mathcal{H}$	**0.9532**	0.9393	**0.8916**	0.8840	**0.4225**	0.3691
$\mathcal{S}$	0.7985	**0.6211**	0.8545	**0.8311**	**0.4120**	0.4473
$\mathcal{U}$	0.1315	**0.2210**	0.0016	**0.0064**	**0.2901**	0.2362
$\mathcal{T}$	2696	**991**	3798	**1052**	4245	**2318**

Table 5
Information regarding the averaged performance over five runs of the hybrid optimization process for simulations of 100 and 200 generations. For these tests, the population size was increase to 100 for the surrogate-based MOEA execution stage.

Metric	Scenario *OptS1*		Scenario *OptS2*		Scenario *OptS3*	
	HybridOpt 100	HybridOpt 200	HybridOpt 100	HybridOpt 200	HybridOpt 100	HybridOpt 200
$\mathcal{H}$	0.9534	0.9535	0.9053	0.9114	0.3910	0.4082
$\mathcal{S}$	0.6103	0.5896	0.7442	0.6814	0.3981	0.3912
$\mathcal{U}$	0.2608	0.1799	0.0198	0.0146	0.1863	0.1790
$\mathcal{T}$	1332	1968	1156	1375	3315	3631

to optimize the number of FE simulations which are required in order to maintain or even to improve the performance of a regression model.

(ii) Implementing a similarity analysis mechanism that will help to further speed-up the optimization process. We wish to group together similar individuals that are to be re-evaluated using FE-simulations and to perform the fitness function calculation only for one representative of each group (e.g. the cluster center). Another option is to directly estimate the fitness of individuals based on similarity analysis [48] or to estimate the fitness of those individuals with a low associated reliability measure, as successfully achieved and verified in [49]. This should drastically reduce the time allocated to re-evaluating promising individuals found during the surrogate-based MOEA execution stage.

Acknowledgements

This work was conducted in the frame of the research program at the Austrian Center of Competence in Mechatronics (ACCM), a part of the COMET K2 program of the Austrian government. The work-related projects are kindly supported by the Austrian government, the Upper Austrian government and the Johannes Kepler University Linz. The authors thank all involved partners for their support. This publication reflects only the authors' views.

References

[1] Electric Motor Systems Annex EMSA, Website http://www.motorsystems.org.

[2] H. De Keulenaer, R. Belmans, E. Blaustein, D. Chapman, A. De Almeida, B. De Wachter, P. Radgen, Energy efficient motor driven systems, Tech. rep., European Copper Institute (2004).

[3] European Union, Regulation (eg) nr. 640/2009.

[4] R. Chiong (Ed.), Nature-Inspired Algorithms for Optimisation, Vol. 193 of Studies in Computational Intelligence, Springer, 2009.

[5] R. Chiong, T. Weise, Z. Michalewicz (Eds.), Variants of Evolutionary Algorithms for Real-World Applications, Springer, 2012.

[6] T. Johansson, M. Van Dessel, R. Belmans, W. Geysen, Technique for finding the optimum geometry of electrostatic micromotors, IEEE Transactions on Industry Applications 30 (4) (1994) 912–919.

[7] K.-Y. Hwang, S.-B. Rhee, J.-S. Lee, B.-I. Kwon, Shape optimization of rotor pole in spoke type permanent magnet motor for reducing partial demagnetization effect and cogging torque, in: IEEE International Conference on Electrical Machines and Systems (ICEMS 2007), 2007, pp. 955–960.

[8] N. Bianchi, S. Bolognani, Design optimization of electric motors by genetic algorithms, IEE Proceedings of Electric Power Applications 145 (5) (1998) 475–483.

[9] X. Jannot, J. Vannier, C. Marchand, M. Gabsi, J. Saint-Michel, D. Sadarnac, Multiphysic modeling of a high-speed interior permanent-magnet synchronous machine for a multiobjective optimal design, IEEE Transactions on Energy Conversion 26 (2) (2011) 457 –467.

[10] Y. del Valle, G. Venayagamoorthy, S. Mohagheghi, J.-C. Hernandez, R. Harley, Particle swarm optimization: Basic concepts, variants and applications in power systems, IEEE Transactions on Evolutionary Computation 12 (2) (2008) 171–195.

[11] S. Russenschuck, Mathematical optimization techniques for the design of permanent magnet synchronous machines based on numerical field calculation, IEEE Transactions on Magnetics 26 (2) (1990) 638–641.

[12] Y. Duan, R. Harley, T. Habetler, Comparison of particle swarm optimization and genetic algorithm in the design of permanent magnet motors, in: IEEE Internationnal Conference on Power Electronics and Motion Control Conference (IPEMC 2009), 2009, pp. 822–825.

[13] Y. Duan, D. Ionel, A review of recent developments in electrical machine design optimization methods with a permanent magnet synchronous motor benchmark study, in: IEEE Energy Conversion Congress and Exposition (ECCE 2011), 2011, pp. 3694–3701.

[14] S. Skaar, R. Nilssen, A state of the art study: Genetic optimization of electric machines, in: IEEE Conference on Power Electronics and Applications (EPE 2003), 2003.

[15] K. Deb, A. Pratap, S. Agarwal, T. Meyarivan, A fast and elitist multiobjective genetic algorithm: NSGA-II, IEEE Transactions on Evolutionary Computation 6 (2) (2002) 182–197.

[16] L. V. Santana-Quintero, A. A. Montao, C. A. C. Coello, A review of techniques for handling expensive functions in evolutionary multi-objective optimization, in: Y. Tenne, C.-K. Goh, L. M. Hiot, Y. S. Ong (Eds.), Computational Intelligence in Expensive Optimization Problems, Vol. 2 of Adaptation, Learning, and Optimization, Springer, 2010, pp. 29–59.

[17] N. Queipo, R. Haftka, W. Shyy, T. Goel, R. Vaidyanathan, P. Kevin Tucker, Surrogate-based analysis and optimization, Progress in Aerospace Sciences 41 (1) (2005) 1–28.

[18] A. Forrester, A. Sobester, A. Keane, Engineering Design via Surrogate Modelling: A Practical Guide, Wiley, 2008.

[19] Y. Tenne, C. Goh (Eds.), Computational Intelligence in Expensive Optimization Problems, Vol. 2 of Adaptation, Learning and Optimization, Springer, 2010.

[20] S. Haykin, Neural Networks: A Comprehensive Foundation, 2nd Edition, Prentice Hall Inc., 1999.

[21] K. Hornik, M. Stinchcombe, H. White, Multilayer feedforward networks are universal approximators, Neural Networks 2 (5) (1989) 359–366.

[22] M. Paliwal, U. A. Kumar, Neural networks and statistical techniques: A review of applications, Expert Systems with Applications 36 (1) (2009) 2–17.

[23] Y. Jin, M. Hüsken, M. Olhofer, B. Sendhoff, Neural networks for fitness approximation in evolutionary optimization, in: Y. Jin (Ed.), Knowledge Incorporation in Evolutionary Computation, Studies in Fuzziness and Soft Computing, Springer, 2004, pp. 281–305.

[24] Y.-S. Hong, H. Lee, M.-J. Tahk, Acceleration of the convergence speed of evolutionary algorithms using multi-layer neural networks, Engineering Optimization 35 (1) (2003) 91–102.

[25] C. N. Gupta, R. Palaniappan, S. Swaminathan, S. M. Krishnan, Neural network classification of homomorphic segmented heart sounds, Applied Soft Computing 7 (1) (2007) 286–297.

[26] A. Wefky, F. Espinosa, A. Prieto, J. Garcia, C. Barrios, Comparison of neural classifiers for vehicles gear estimation, Applied Soft Computing 11 (4) (2011) 3580–3599.

[27] R. Collobert, S. Bengio, SVMTorch: Support vector machines for large-scale regression problems, Journal of Machine Learning Research 1 (2001) 143–160.

[28] M. Buhmann, Radial Basis Functions: Theory and Implementations, Cambridge University Press, 2003.

[29] D. Aha, D. Kibler, M. Albert, Instance-based learning algorithms, Machine learning 6 (1) (1991) 37–66.

[30] FEMAG - The finite-element program for analysis and simulation of electrical machines and devices, Website http://people.ee.ethz.ch/∼ femag/englisch/index_en.htm.

[31] K. Deb, Multi-Objective Optimization using Evolutionary Algorithms, John Wiley & Sons, 2001.

[32] E. Zitzler, M. Laumanns, L. Thiele, SPEA2: Improving the strength Pareto evolutionary algorithm for multiobjective optimization, in: Evolutionary Methods for Design, Optimisation and Control with Application to Industrial Problems (EUROGEN 2001), International Center for Numerical Methods in Engineering (CIMNE), 2002, pp. 95–100.

[33] V. Khare, X. Yao, K. Deb, Performance scaling of multi-objective evolutionary algorithms, in: International Conference on Evolutionary Multi-Criterion Optimization (EMO 2003), Springer, 2003, pp. 376–390.

[34] L. Raisanen, R. M. Whitaker, Comparison and evaluation of multiple objective genetic algorithms for the antenna placement problem, Mobile Networks Applications 10 (2005) 79–88.

[35] S. Anauth, R. Ah King, Comparative application of multi-objective evolutionary algorithms to the voltage and reactive power optimization problem in power systems, in: International Conference on Simulated Evolution And Learning (SEAL 2010), Springer, 2010, pp. 424–434.

[36] P. J. Werbos, Beyond regression: New tools for prediction and analysis in the behavioral sciences, Ph.D. thesis, Harvard University (1974).

[37] P. S. Churchland, T. J. Sejnowski, The Computational Brain, MIT Press, 1992.

[38] G. Cybenko, Approximation by superpositions of a sigmoidal function, Mathematics of Control, Signals, and Systems 2 (4) (1989) 303–314.

[39] L. Breiman, J. Friedman, R. Olshen, C. Stone, Classification and Regression Trees, Chapman and Hall / CRC, 1993.

[40] T. Hastie, R. Tibshirani, J. Friedman, The Elements of Statistical Learning: Data Mining, Inference and Prediction, 2nd Edition, Springer, 2009.

[41] J. J. Durillo, A. J. Nebro, JMETAL: A Java framework for multi-objective optimization, Advances in Engineering Software 42 (2011) 760–771.

[42] M. Hall, E. Frank, G. Holmes, B. Pfahringer, P. Reutemann, I. H. Witten, The WEKA data mining software: an update, SIGKDD Explorations 11 (1) (2009) 10–18.

[43] E. Zitzler, Evolutionary algorithms for multiobjective optimization: Methods and applications, Ph.D. thesis, Swiss Federal Institute of Technology (1999).

[44] A. Zhou, Y. Jin, Q. Zhang, B. Sendhoff, E. Tsang, Combining model-based and genetics-based offspring generation for multi-objective optimization using a convergence criterion, in: IEEE Congress on Evolutionary Computation (CEC 2006), 2006, pp. 892–899.

[45] M. Fleischer, The measure of Pareto optima. applications to multi-objective metaheuristics, in: International Conference on Evolutionary Multi-Criterion Optimization (EMO 2003), Springer, 2003, pp. 519–533.

[46] E. Lughofer, P. Angelov, Handling drifts and shifts in on-line data streams with evolving fuzzy systems, Applied Soft Computing 11 (2) (2011) 2057–2068.

[47] E. Lughofer, Single-pass active learning with conflict and ignorance, Evolving Systems 3 (4) (2012) 251–271.

[48] M. Salami, T. Hendtlass, The fast evaluation strategy for evolvable hardware, Genetic Programming and Evolvable Machines 6 (2) (2005) 139–162.

[49] M. Salami, T. Hendtlass, A fast evaluation strategy for evolutionary algorithms, Applied Soft Computing 2 (3) (2003) 156–173.

[50] K. Deb, R. B. Agrawal, Simulated binary crossover for continuous search space, Complex Systems 9 (1995) 115–148.

[51] K. Deb, M. Goyal, A combined genetic adaptive search (GeneAS) for engineering design, Computer Science and Informatics 26 (1996) 30–45.

Appendix A. Appendix: An Overview of the NSGA-II Algorithm

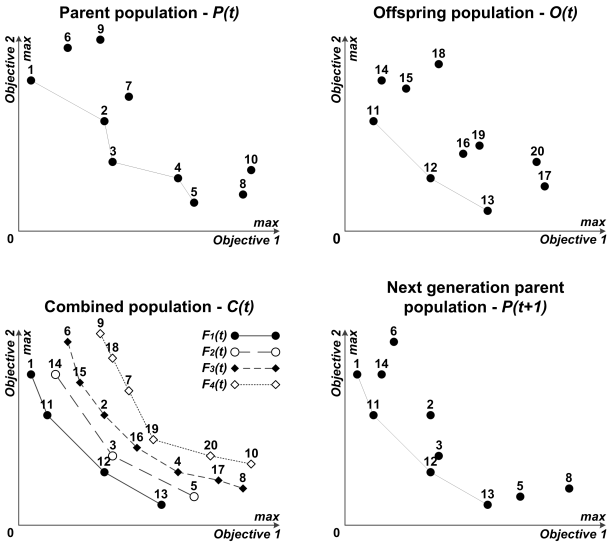

Fig. A.1. Example of the evolution of a population of size 10 in NSGA-II when considering a MOOP with two objectives

NSGA-II stores at each generation t two distinct populations of the same size n, a parent population $P(t)$ and an offspring population $O(t)$. Population $P(t+1)$ is obtained by selecting the best n individuals from the combined populations of the previous generation, i.e., from $C(t) = P(t) \cup O(t)$. The fitness of an individual is assessed by using two metrics. The first metric is a classification of the individuals in the population into non-dominated fronts. The first front $F_1(t)$ is the highest level Pareto front and contains the Pareto optimal set from $C(t)$. The subsequent lower-level fronts $F_j(t), j > 1$ are obtained by removing higher level Pareto fronts from the population and extracting the Pareto optimal set from the remaining individuals, i.e., $F_j(t), j > 1$ contains the Pareto optimal set from $C(t) \setminus \bigcup_{k=1}^{j-1} F_k(t)$. Individuals in a higher-level front $F_j(t)$ are ranked as having a higher fitness than individuals in a lower-level front $F_{j+1}(t)$. NSGA-II uses a second metric, the crowding distance, in order to rank the quality of individuals from the same front. The crowding distance [15] associated to a certain individual is an indicator of how dense the non-dominated front is around that respective individual.

Population $P(t+1)$ is constructed by adding individuals from the higher non-dominated fronts, starting with $F_1(t)$. If a front is too large to be added completely, ties are broken in favor of the individuals that have the higher crowding distance, i.e., that are located in a less crowded region of the front. The full mechanism through which population $P(t+1)$ is obtained from population $P(t)$ is illustrated in Figure A.1. Population $O(t+1)$ is obtained from population $P(t+1)$ by using binary tournament selection, simulated binary crossover [50] and polynomial mutation [51].